*J. Fluid Mech.* (1975), *vol.* 72, *part* 1, *pp.* 95–112
*Printed in Great Britain*


# Electrohydrostatic instability in electrically stressed dielectric fluids. Part 2

By D. H. MICHAEL, J. NORBURY AND M. E. O'NEILL
Department of Mathematics, University College London

With an appendix by D. H. MICHAEL and M. E. O'NEILL

(Received 8 January 1975)

The paper is the second part of a study of the failure of the insulation of a layer of dielectric fluid of arbitrary volume, occupying a hole in a solid dielectric sheet, when stressed by an applied electric field. In part 1 symmetric and asymmetric equilibria were found for the two-dimensional problem, using an approximation given by Taylor (1968) for the electric field, which is valid for large holes. In this paper axisymmetric equilibria are given for a circular hole, under the same conditions. In addition the points of bifurcation of asymmetric solutions have been found, and provide sufficient information to give the stability characteristics. It is found that when the volume-excess fraction $\delta$ exceeds a value of approximately $-0{\cdot}3$ instability occurs in an asymmetric form reported earlier for large holes by Michael, O'Neill & Zuercher (1971) in the case $\delta = 0$. For $\delta < -0{\cdot}3$ the nature of the instability changes to an axisymmetric form of failure associated with a maximum of the loading parameter.

The analysis given shows that axisymmetric displacements of 'sausage' mode type, that is, symmetric about a centre-plane, are associated with small changes in the static pressure in the dielectric layer. Such modes have not previously been examined in this context, and in an appendix to this paper Michael & O'Neill give an analysis of them when $\delta = 0$, valid for all hole sizes, by extending the small perturbation analysis of Michael, O'Neill & Zuercher. These modes however do not provide the most unstable displacements for any configuration, and do not therefore affect the stability from a physical point of view.

## 1. Introduction

This paper is a sequel to a paper by Michael, Norbury & O'Neill (1974, called part 1). The work arises from an earlier study made by Michael, O'Neill & Zuercher (1971), hereafter referred to as MONZ, of the failure of the insulation of a dielectric fluid filling a circular hole in a solid dielectric sheet when the fluid is stressed by an electric field. In part 1 the authors initiated a discussion of the problem when such a hole is partially filled, and it was shown that for wide holes a formulation similar to that given by Taylor (1968) could be used. Some consequences of the analysis for a circular hole were given in the introduction of part 1, but detailed discussion and results were there given for the two-dimensional plane problem only. The purpose of the present paper is therefore to give an account of the results which have been obtained for the instability of a partially filled circular hole.

It will be assumed here that the reader is familiar with the notation and the formulation of the problem given in the introduction of part 1. The central problem which is posed for a circular hole is to solve the boundary-value problem

$$\left.\begin{aligned}\frac{\partial^2 y}{\partial x^2}+\frac{1}{x}\frac{\partial y}{\partial x}+\frac{1}{x^2}\frac{\partial^2 y}{\partial \theta^2} = \alpha+\frac{\beta}{y^2} \quad (0 \leqslant x \leqslant 1, \quad 0 \leqslant \theta < 2\pi),\\ y(x,\theta) \geqslant 0, \quad \beta \geqslant 0,\end{aligned}\right\} \tag{1}$$

with the condition $y = 1$ at $x = 1$ $(0 \leqslant \theta < 2\pi)$, and to obtain the loci in the $\alpha$, $\beta$ plane for which the solutions give a prescribed value for the volume excess $\delta$.

When $\delta = 0$ there exists the axisymmetric solution $y \equiv 1$, for which $\alpha+\beta = 0$, and the stability of this equilibrium was the subject of analysis in MONZ. It was shown there that for wide holes the instability of primary interest, that is, the instability appearing at the lowest level of the applied electric field, is an asymmetric 'sausage' mode. This suggests that, for given $\delta \neq 0$, we should study first of all the axisymmetric solutions of (1). Second, we need to ascertain points of bifurcation of the axisymmetric solutions into asymmetric solutions. We begin with a discussion of the axisymmetric solutions.

## 2. Axisymmetric solutions

For these solutions the boundary-value problem (1) is reduced to

$$\left.\begin{aligned}\frac{d^2 y}{dx^2}+\frac{1}{x}\frac{dy}{dx} = \alpha+\frac{\beta}{y^2} \quad (0 \leqslant x \leqslant 1),\\ y = 1 \quad \text{at} \quad x = 1.\end{aligned}\right\} \tag{2}$$

Also, for smooth solutions in this case, $dy/dx = 0$ at $x = 0$.

We require values of $\alpha$ and $\beta$ for which this problem has a solution which satisfies the volume constraint equation

$$2\pi\int_0^1 xy\,dx-\pi = \delta, \tag{3}$$

where $\delta$ is initially prescribed.

Solutions of (2) were given by Taylor (1968) and Ackerberg (1969), for prescribed values of $\alpha$. If $y_0$ is the value of $y$ at the centre $x = 0$, such solutions plotted in the $y_0$, $\beta$ plane are typically as shown in figure 1, each point of a curve representing a solution of (2) for a prescribed value of $\alpha$.

Starting with $\beta = 0$, a stable equilibrium may be followed up each curve as the applied field strength is increased until the first maximum of the curve is reached; this represents the value of $\beta$ at which the equilibrium becomes unstable. It can be seen that these curves subsequently develop an infinite number of oscillations as they approach a limit point $\beta = \beta_0$ as $y_0 \to 0$. In the case when $\alpha = 0$ this process was described in detail by Ackerberg, using a phase-plane transformation in which it was shown that this limit point is a spiral point. Unfortunately there appears to be no similar extension of this analysis when $\alpha \neq 0$. However, we are able to find the limiting value $\beta_0$ for any value of $\alpha$. Solutions with $\beta = \beta_0$ have a cuspidal behaviour at $x = 0$.

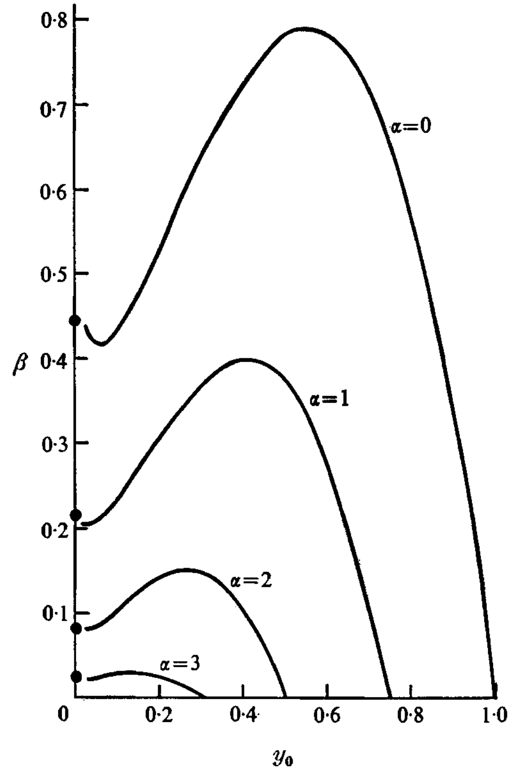


FIGURE 1. The loci of axisymmetric equilibrium solutions at constant $\alpha$, after Taylor (1968) and Ackerberg (1969). ●, limiting cuspidal spiral-point solution as $y_0 \to 0$.

When $\alpha = 0$ Ackerberg gave the value $\beta_0 = \frac{4}{9}$. This can be verified by looking for a solution of (2) when $\alpha = 0$ of the form $y = \lambda x^k$. It follows by substitution that $k = \frac{2}{3}$ and $\lambda^3 = \frac{9}{4}\beta$. Hence, with $y = 1$ at $x = 1$, we require $\beta_0 = \frac{4}{9}$, and the limiting solution is then $y = x^{\frac{2}{3}}$.

When $\alpha \neq 0$ the cuspidal form of the solution at $x = 0$ will not be affected since as $y \to 0$, $\alpha y^2/\beta \to 0$. Hence we write $y = ax^{\frac{2}{3}}z(x)$, where $z(0) \neq 0$. Substitution into (2) shows easily that when $a$ is chosen to make $z(0) = 1$, $a^3 = \frac{9}{4}\beta$ and $z(x)$ satisfies the equation

$$\frac{9}{4}\left(x^2\frac{d^2z}{dx^2}+\frac{7}{3}x\frac{dz}{dx}\right)+z-\frac{1}{z^2} = \frac{\alpha}{\beta}\left(\frac{9\beta}{4}\right)^{\frac{2}{3}}x^{\frac{4}{3}}.$$

A solution in powers of $x^{\frac{4}{3}}$ is appropriate. If we write $\xi = (\alpha/\beta)\,(\frac{9}{4}\beta)^{\frac{2}{3}}x^{\frac{4}{3}}$ the boundary-value problem becomes

$$4\xi^2\frac{d^2z}{d\xi^2}+8\xi\frac{dz}{d\xi}+z-\frac{1}{z^2} = \xi, \tag{4}$$

with $z = 1$ at $\xi = 0$ and $z = (4/9\beta)^{\frac{1}{3}}$ at $\xi = \alpha/\beta(\frac{9}{4}\beta)^{\frac{2}{3}}$.

A power-series solution of (4) appropriate for small $\xi$ has the form

$$z = 1+\frac{\xi}{11}+\frac{\xi^2}{1089}-\frac{10}{153\times 11^3}\xi^3+\dots.$$

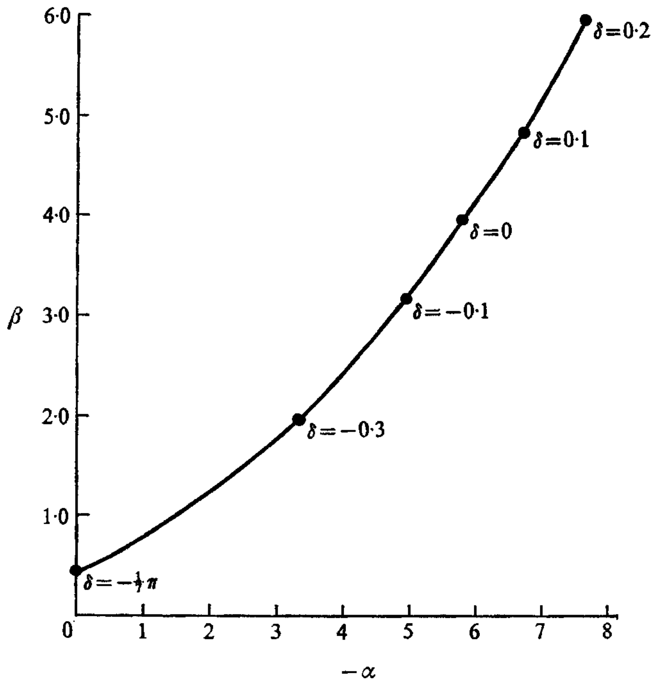


FIGURE 2. The locus of spiral-point solutions in the $\alpha$, $\beta$ plane.

This power series was used to initiate a numerical solution of (4) for larger values of $\xi$. It follows that, by assigning a value $\beta = \beta_0$ at the limit point, the corresponding value of $\alpha$ is obtained from the solution of (4) by finding the value of $\xi = \alpha/\beta_0(\frac{9}{4}\beta_0)^{\frac{2}{3}}$ at which $z = (4/9\beta_0)^{\frac{1}{3}}$. We are thus able to obtain the locus of these limit points in the $\alpha$, $\beta$ plane. It will be clear from the discussions in part 1 that we are interested in correlating these solutions with the volume excess $\delta$. In terms of $\xi$,

$$\delta = \frac{2\pi}{3}\frac{\beta}{\alpha^2}\int_0^k \xi z(\xi)\, d\xi - \pi,$$

where $k = \alpha/\beta(\frac{9}{4}\beta)^{\frac{2}{3}}$. This formula enables us to calculate $\delta$ at each limit point in the $\alpha$, $\beta$ plane. Figure 2 gives the locus of these cuspidal limit-point solutions with typical values of $\delta$ shown. It is interesting to note that cusps of this form cannot occur in axisymmetric solutions, for finite $\beta$, except at the centre $x = 0$. Any such solution with a cusp occurring at $x = x_0$ $(0 < x_0 < 1)$ will be a ring cusp, and will be governed by the equation

$$\frac{d^2y}{d\eta^2} + \frac{1}{x_0}\frac{dy}{d\eta} = \frac{\beta}{y^2}$$

as $y \to 0$, when $x = x_0 + \eta$. With $d^2y/d\eta^2$ the dominant term on the left-hand side, the solution must take the limiting form $y = -(\frac{9}{4}\beta)^{\frac{1}{3}}\eta^{\frac{2}{3}}$ as $\eta \to 0$, which is inadmissible since $y < 0$.

It was shown in part 1 that, when $\beta \to 0$, piecewise smooth solutions, in which $dy/dx$ changes sign at the points where $y = 0$, can be found in the two-dimensional problem. Similar solutions occur in the axisymmetric problem as $\beta \to 0$. For example a solution smooth at $x = 0$ with $y = 0$ at $x = x_0$ is given by

$$y = \begin{cases} \frac{1}{4}\alpha(x^2 - x_0^2) & (0 \leqslant x \leqslant x_0), \\ 1 + \frac{1}{4}\alpha(x^2-1) - [1 + \frac{1}{4}\alpha(x_0^2 - 1)]\log x/\log x_0 & (x_0 \leqslant x \leqslant 1). \end{cases}$$

To specify the connexion between $\alpha$ and $x_0$, it can easily be seen that the slopes of the two branches at $x = x_0$ must be equal and opposite. This is the same condition as that applying in part 1, and indicates that such 'corner' solutions are locally two-dimensional near $y = 0$.

A feature of the axisymmetric solutions which helps in the understanding of the results is that smooth profiles cannot change from having a maximum to having a minimum of $y$ at $x = 0$, or vice versa. For, if such a transition were to take place, $dy/dx = 0$ and $d^2y/dx^2 = 0$ at $x = 0$, and solutions of (2) for small $x$ would be of the form $y = a_0 + a_4x^4 + a_6x^6 + \ldots$. Substitution into (2) shows that $a_4 = a_6 = a_8 = \ldots = 0$. Hence the only solution satisfying the condition is $y \equiv 1$, occurring as part of the $\delta = 0$ locus. Thus the loci of solutions, for given $\delta \neq 0$, must divide into two unconnected sections with a maximum and a minimum in the profile at $x = 0$, respectively.

Another feature of interest in axisymmetric solutions is that no bifurcation of a locus for prescribed $\delta \neq 0$ in the $\alpha, \beta$ plane will occur. For, suppose such a bifurcation were to occur at a point $(\alpha_0, \beta_0)$ where the solution is $y = f_0(x)$. Hence

$$\frac{d^2f_0}{dx^2} + \frac{1}{x}\frac{df_0}{dx} = \alpha_0 + \frac{\beta_0}{f_0^2},$$

where $df_0/dx = 0$ at $x = 0$, $f_0 = 1$ at $x = 1$ and

$$\delta = 2\pi \int_0^1 (f_0(x) - 1)\, x\, dx$$

has a prescribed value. If $y = f_0 + f_1$, $\alpha = \alpha_0 + \alpha_1$, $\beta = \beta_0 + \beta_1$ is a perturbation in which quantities with a suffix 1 denote first-order changes, then

$$\frac{d^2f_1}{dx^2} + \frac{1}{x}\frac{df_1}{dx} + \frac{2\beta_0}{f_0^3}f_1 = \alpha_1 + \frac{\beta_1}{f_0^2},$$

with $df_1/dx = 0$ at $x = 0$, $f_1 = 0$ at $x = 1$ and

$$\int_0^1 xf_1\, dx = 0.$$

At a point of bifurcation there will be two solutions $f_{11}$ and $f_{12}$ satisfying these perturbation conditions with perturbations in $(\alpha, \beta)$ given by $(\alpha_{11}, \beta_{11})$ and $(\alpha_{12}, \beta_{12})$ respectively. In such a case it would follow, by taking a linear combination $pf_{11} + qf_{12}$ of $f_{11}$ and $f_{12}$, that a perturbation $\alpha_1^* = p\alpha_{11} + q\alpha_{12}, \beta_1^* = p\beta_{11} + q\beta_{12}$ in any direction would be attainable. Thus uniquely defined bifurcations cannot exist, with the one exception of when $\delta = 0, f_0(x) \equiv 1$ and $\alpha_0 + \beta_0 = 0$. In this case one of the perturbations is along the straight line $\alpha + \beta = 0$, and for this the perturbation equation has solution $f_{11} \equiv 0$, with $\alpha_{11} + \beta_{11} = 0$. Thus uniquely defined bifurcations from the line $\alpha + \beta = 0$ can and do occur on the $\delta = 0$ locus.

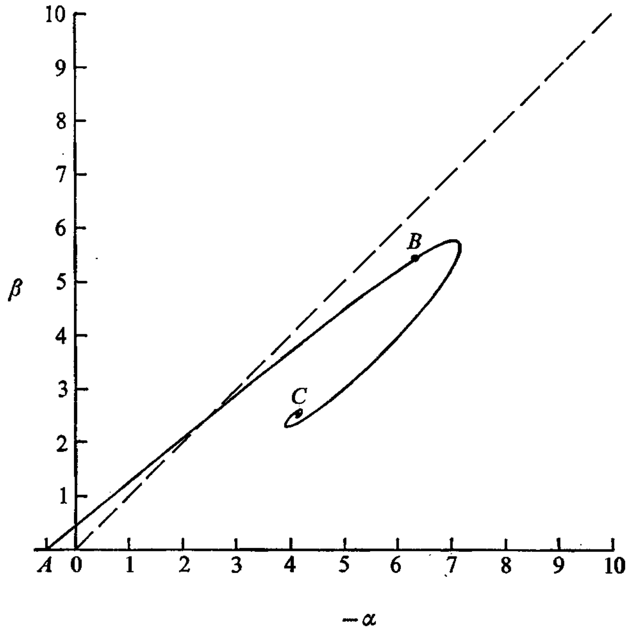


FIGURE 3. The first branch of the locus of symmetric equilibria in the $\alpha$, $\beta$ plane for $\delta = -0{\cdot}2$. $A$ is the initial unstressed state. $B$ is the point of asymmetric bifurcation. $C$ is the spiral-point limit. The $\delta = 0$ line, $\alpha+\beta = 0$, is marked dashed for comparison.

Our final remarks on the axisymmetric solutions concern the numerical computation. For this purpose it is convenient to scale out the parameter $\alpha$ from (2). Since negative values of $\alpha$ are of most interest, for $\alpha < 0$ we write $x' = (-\alpha)^{\frac{1}{2}}x$, and write (2) as

$$\frac{d^2y}{dx'^2}+\frac{1}{x'}\frac{dy}{dx'} = -1+\frac{\gamma}{y^2}, \tag{5}$$

where $\gamma = -\beta/\alpha > 0$. The boundary conditions are then $dy/dx' = 0$ at $x' = 0$ and $y = 1$ at $x' = (-\alpha)^{\frac{1}{2}}$. The method of computation was to assign a value of $\gamma$ and to compute the solution of (5) with $dy/dx' = 0$ and $y = y_0$ at $x = 0$, where $y_0$ takes on consecutively a range of positive values. The value of $\alpha$ is then found by finding the value of $x' = (-\alpha)^{\frac{1}{2}}$ at which $y = 1$. The value of $\beta$ then follows since $\beta = -\alpha\gamma$. For each such solution the value of $\delta$ is obtained by numerical integration from the formula

$$\delta = 2\pi\int_0^1 x(y-1)\,dx = -2\pi\alpha\int_0^{(-\alpha)^{\frac{1}{2}}} x'(y-1)\,dx'.$$

The program is then arranged to search for solutions which have a prescribed value of $\delta$. Loci of symmetric solutions were obtained in this way for $\delta = -0{\cdot}2$, 0 and $+0{\cdot}2$, and the branches which are of most interest are shown in figures 3–5. These results confirm the properties of the solutions mentioned above. Only in the case $\delta = 0$ is there a bifurcation of the symmetric loci. The property that centre-up solutions are unconnected with centre-down solutions is illustrated by

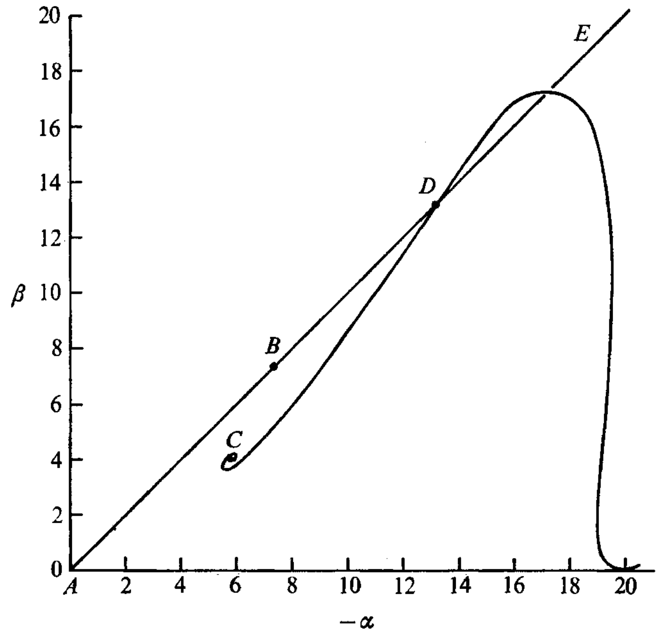


FIGURE 4. The locus of symmetric equilibria in the $\alpha$, $\beta$ plane for $\delta = 0$. $A$ is the initial unstressed state. $B$ is the first point of asymmetric bifurcation. $C$ is the spiral-point limit. $D$ is the first symmetric bifurcation point from the line $\alpha+\beta = 0$.

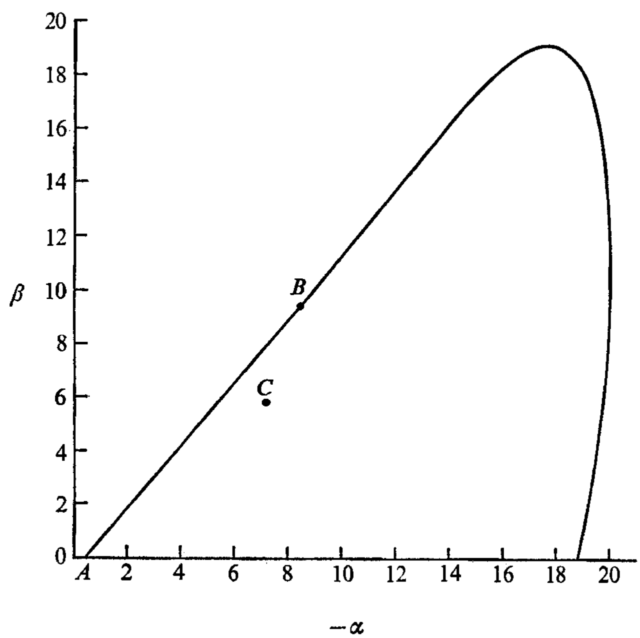


FIGURE 5. The first branch of the locus of symmetric equilibria in the $\alpha$, $\beta$ plane for $\delta = +0{\cdot}2$. $A$ is the initial unstressed state. $B$ is the point of asymmetric bifurcation. $C$ is the spiral point, which is an end point of another branch of the locus (not given) unconnected with the initial state $A$.

the difference in behaviour for $\delta > 0$ and $\delta < 0$. For $\delta < 0$ the first loop of the locus, beginning with the unstressed state $A$, which is a centre-down profile, ends on the spiral point of the cuspidal solution. For $\delta > 0$ the initial state $A$ has a centre-up profile, and is unconnected with the spiral point. In this case the spiral point is an end point of a separate locus of centre-down solutions. But since this has no bearing on the instability criteria, it was not thought worthwhile to follow this locus for $\delta > 0$.

## 3. Asymmetric solutions

It was pointed out in part 1 that the analysis of MONZ for large holes, in the case $\delta = 0$, shows that instability first occurs in non-axisymmetric modes. For this reason it is important to obtain some knowledge of the non-axisymmetric solutions of the boundary-value problem (1). However, solutions of (1) are difficult to obtain analytically, and numerical solutions which are not axisymmetric are also difficult to obtain because of the non-uniqueness of the solutions of (1) for given $\alpha$ and $\beta$. We have therefore endeavoured to determine those features of the asymmetric solutions which are of principal interest and which, as we shall show, are obtainable from the solution of a well-posed numerical problem requiring only a small amount of additional computation.

It can be seen, by analogy with the two-dimensional analysis of part 1, that the most important points to obtain in the $\alpha, \beta$ plane are the first points of bifurcation of asymmetric solution loci from symmetric solution loci for given $\delta$. The latter having already been obtained, a limited test program can be devised to identify these bifurcations.

Let $y = f_0(x)$ be a smooth axisymmetric solution of (1) at $(\alpha_0, \beta_0)$, satisfying the equation

$$\frac{d^2 f_0}{dx^2} + \frac{1}{x}\frac{df_0}{dx} = \alpha_0 + \frac{\beta_0}{f_0^2}$$

and the boundary conditions $f_0(1) = 1$ and $df_0/dx = 0$ at $x = 0$. To obtain asymmetric bifurcations, consider a small smooth perturbation in which

$$y = f_0(x) + f_1(x, \theta), \quad \alpha = \alpha_0 + \alpha_1, \quad \beta = \beta_0 + \beta_1,$$

where, again, quantities with a suffix 1 are small first-order perturbations. Substitution in (1) shows that

$$\frac{\partial^2 f_1}{\partial x^2} + \frac{1}{x}\frac{\partial f_1}{\partial x} + \frac{1}{x^2}\frac{\partial^2 f_1}{\partial \theta^2} + \frac{2\beta_0}{[f_0(x)]^3} f_1 = \alpha_1 + \frac{\beta_1}{[f_0(x)]^2}, \tag{6}$$

and that $f_1 = 0$ at $x = 1$ $(0 \leqslant \theta < 2\pi)$. Solutions of (6) may be written as $f_1(x, \theta) = g_1(x) + h_1(x, \theta)$, in which $g_1(x)$ is a particular integral satisfying the equation

$$\frac{d^2 g_1}{dx^2} + \frac{1}{x}\frac{dg_1}{dx} + \frac{2\beta_0}{[f_0(x)]^3} g_1 = \alpha_1 + \frac{\beta_1}{[f_0(x)]^2}, \tag{7}$$

and $h_1(x, \theta)$ is a complementary function for which

$$\frac{\partial^2 h_1}{\partial x^2} + \frac{1}{x}\frac{\partial h_1}{\partial x} + \frac{1}{x^2}\frac{\partial^2 h_1}{\partial \theta^2} + \frac{2\beta_0}{[f_0(x)]^3} h_1(x, \theta) = 0. \tag{8}$$

Single-valued solutions of (8) can be written in terms of the Fourier constituents $k_{1m}(x) \,{}^{\sin}_{\cos}\, m\theta$, where $m$ is an integer. The bifurcation of principal interest occurs when $m = 1$. Thus we write

$$f_1(x, \theta) = g_1(x) + k_{11}(x) \,{}^{\sin}_{\cos}\, \theta,$$

in which $g_1(1) = 0$ and $k_{11}(1) = 0$. The requirement that $g_1(x)$ shall be smooth at $x = 0$, together with the condition $g_1(1) = 0$, determines the solution of (7) for $g_1(x)$, in terms of $\alpha_1$ and $\beta_1$. The further requirement that the volume of fluid occupying the hole is unchanged in the perturbation applies to the solution $g_1(x)$ since the second term of $f_1$ does not contribute to any change in volume. It is not necessary to pursue this condition further, but it will evidently give rise to a connexion between $\alpha_1$ and $\beta_1$. This however is simply the continuation of the locus of axisymmetric solutions. Of more interest here is the second term of $f_1$, representing a bifurcation away from the symmetric locus. In this term $k_{11}(x)$ clearly must satisfy the equation

$$\frac{d^2k_{11}}{dx^2} + \frac{1}{x}\frac{dk_{11}}{dx} - \frac{k_{11}}{x^2} + \frac{2\beta_0}{[f_0(x)]^3}k_{11} = 0, \tag{9}$$

with $k_{11}(1) = 0$ and $k_{11}(x)$ regular at $x = 0$. Now $f_0(x)$ is an even function of $x$ which is regular at $x = 0$ and $f_0(0) \neq 0$. Hence the last term on the left-hand side of (9) does not contribute to the singularity of the equation at $x = 0$. The solution regular at $x = 0$ is thus of the form $k_{11} = x + a_3 x^3 + a_5 x^5 + \ldots$. The satisfaction of the boundary-value problem (9), by $k_{11}(x)$, provides a simple test for the first asymmetric bifurcation. This test can be incorporated conveniently into the program for finding the symmetric solution loci in the $\alpha, \beta$ plane for prescribed $\delta$. Having established a point on the locus the appropriate value of $\beta_0$ and the profile $f_0(x)$ can be put into (9) and a numerical integration of the equation forward to $x = 1$ establishes the value of $k_{11}(1)$. The first bifurcation point occurs where $k_{11}(1)$ first becomes zero. In figures 3–5, the points labelled $B$ show this bifurcation point for the values $\delta = -0{\cdot}2$, 0 and $+0{\cdot}2$.

Without recourse to much more extensive computation we are unable to obtain the loci of asymmetric solutions as we were able to do in part 1. But some features of these solutions may be deduced. One can, for example, following part 1, look for asymmetric solutions as $\beta \to 0$ having profiles in which $y(x, \theta)$ is singular where $y$ becomes zero. Such a solution will satisfy the equation

$$\frac{\partial^2 y}{\partial x^2} + \frac{1}{x}\frac{\partial y}{\partial x} + \frac{1}{x^2}\frac{\partial^2 y}{\partial \theta^2} = \alpha \quad (y > 0), \tag{10}$$

except at the singular points, where $y = 0$ with $y = 1$ at $x = 1$ $(0 \leqslant \theta < 2\pi)$. The solution of (10) is $y = \frac{1}{4}\alpha x^2 + \tilde{y}(x, \theta)$, where $\tilde{y}(x, \theta)$ is a harmonic function. If it is assumed that there is one isolated point $(x_0, \theta_0)$ at which $y = 0$, we require that $\tilde{y} = 1 - \frac{1}{4}\alpha$, a constant, on $x = 1$ $(0 \leqslant \theta < 2\pi)$ and $\tilde{y} = -\frac{1}{4}\alpha x_0^2$ at $(x_0, \theta_0)$. The solution for $\tilde{y}$ is $\tilde{y} = 1 - \frac{1}{4}\alpha$ at all points except the singular point, where $y = -\frac{1}{4}\alpha x_0^2$. Such a discontinuous limiting solution could not be achieved as the limiting form of a continuous profile, and we conclude that the asymmetric loci of constant $\delta$ will not approach the axis $\beta = 0$ in this way. Similar conclusions clearly follow when there are a finite number of isolated singular points of this kind. However, the case in which $y \to 0$ as $\beta \to 0$ at all points of a closed curve $\Gamma$ within the domain $0 < x < 1$ $(0 \leqslant \theta < 2\pi)$ is different. Here the condition on $\tilde{y}$ is that $\tilde{y} = -\frac{1}{4}\alpha x^2$ at each point of $\Gamma$. Solutions interior to $\Gamma$, and in the part of the domain between $\Gamma$ and the exterior boundary $x = 1$ are then obtainable. Such solutions, representing asymmetric forms of the symmetric 'corner' type solutions discussed earlier, provide a limit by which asymmetric solution loci may descend to the axis $\beta = 0$.

Finally it is natural to inquire whether spiral points can appear in the asymmetric solution loci. These would be associated with off-centre cusp profiles. For such a limiting solution with a cusp at $x = x_0$ $(\neq 0)$ it may be expected that the solution in the immediate neighbourhood of the cusp will become axisymmetric. Thus if $\rho$ is the radius from the cusp point the local behaviour will be governed by the equation

$$\frac{d^2y}{d\rho^2}+\frac{1}{\rho}\frac{dy}{d\rho} = \frac{\beta}{y^2}$$

as $y \to 0$, with the known cusp singularity for which $y \to (\frac{9}{4}\beta)^{\frac{1}{3}}\rho^{\frac{2}{3}}$ as $\rho \to 0$. To find such limiting solutions it is then necessary to solve the boundary-value problem given by (1), with this singularity at the cusp point. This again requires extensive computation, and since it is not necessary to know these limits to establish the stability of the system from a physical point of view, we have not deemed it worthwhile to pursue them further.

## 4. Bifurcations of the $\delta = 0$ locus

The bifurcations occurring when $\delta = 0$ are worthy of special mention for several reasons. They can be directly correlated with the stability results given in MONZ and they can be given explicit mathematical forms. Furthermore this is the only case in which bifurcation from a symmetric locus occurs.

The equilibrium of the fully filled hole is given here by the line $\alpha + \beta = 0$ in the $\alpha$, $\beta$ plane, for which $y(x) \equiv 1$, and the instability considered in MONZ is represented here, for large holes, by the bifurcations from this line. To consider these bifurcations we write

$$y = 1+\zeta_1+\zeta_2+\dots, \quad \alpha = \alpha_0+\alpha_1+\alpha_2+\dots \quad \text{and} \quad \beta = \beta_0+\beta_1+\beta_2+\dots,$$

in which suffixes 1, 2, 3, ... denote first-, second- and third-order perturbations, etc., from the solution $y \equiv 1$, $\alpha_0+\beta_0 = 0$. The first-order equation for $\zeta_1$ becomes

$$\frac{\partial^2\zeta_1}{\partial x^2}+\frac{1}{x}\frac{\partial\zeta_1}{\partial x}+\frac{1}{x^2}\frac{\partial^2\zeta_1}{\partial\theta^2}+m^2\zeta_1 = \alpha_1+\beta_1, \tag{11}$$

where $m^2 = 2\beta_0$. The solution of (11) is required subject to the conditions $\zeta_1 = 0$ on $x = 1$ $(0 \leqslant \theta < 2\pi)$ and

$$\int_{x=0}^{1}\int_{\theta=0}^{2\pi}\zeta_1 x\,dx\,d\theta = 0,$$

this latter equation being the condition of volume conservation. The solution is evidently of the form $\zeta_1 = (\alpha_1+\beta_1)/m^2+\zeta_1^*$, where $\zeta_1^*$ is a complementary function. The first bifurcation occurring is associated with the asymmetric mode in which $\zeta_1^* \propto {\sin \atop \cos}\,\theta$, in which case we have

$$\zeta_1 = (\alpha_1+\beta_1)/m^2 + A_1 J_1(mx) {\sin \atop \cos}\,\theta,$$

where $A_1$ is a first-order constant and $J_1$ is a Bessel function. Here the volume conservation requires that $\alpha_1+\beta_1 = 0$, and the remaining condition requires $J_1(m) = 0$. The first root of this equation is $m = 3{\cdot}832$, giving $\beta_0 = -\alpha_0 = 7{\cdot}35$. The structure of the higher-order terms in this bifurcation is the same as in the two-dimensional case of part 1, and will not be given in detail. At second order we find that $\alpha_1 = \beta_1 = 0$ necessarily, and that the first perturbations of $\alpha_0$ and $\beta_0$ are $\alpha_2$ and $\beta_2$. Second-order analysis establishes the value of $\alpha_2+\beta_2$ in terms of $A_1^2$, and it requires a third-order analysis to give $\alpha_2$ and $\beta_2$ separately. This form of result demonstrates the one-sided nature of this bifurcation. The critical values of $\alpha_0$ and $\beta_0$, given by the point $B$ in figure 4, correspond to those given in MONZ for large circular holes. The next bifurcation from the solution $y \equiv 1$ is the first axisymmetric mode in which

$$\zeta_1 = (\alpha_1+\beta_1)/m^2 + A_1 J_0(mx).$$

With $\zeta_1 = 0$ at $x = 1$ we have

$$\zeta_1 = \frac{\alpha_1+\beta_1}{m^2 J_0(m)}\{J_0(m)-J_0(mx)\}.$$

The volume condition, $$\int_0^1 x\zeta\,dx = 0,$$

then gives $mJ_0(m) = 2J_1(m)$. The lowest root of this equation is $m = 5{\cdot}1$ approximately, and $\beta_0 = -\alpha_0 = 13{\cdot}2$. This is the point $D$ in figure 4. The first appearance of an axisymmetric bifurcation of this kind is not practically significant as it comes at a value of $\beta$ greater than the value at which the first instability occurs. But the appearance of such modes here provides a better understanding of their place in the theory. MONZ considered axisymmetric modes under the condition of constant internal pressure, in which case the axisymmetric sausage mode does not exist. Here we see that such modes can appear with suitable perturbations of the internal static pressure, represented in this theory by an increment $\delta\alpha$ in $\alpha$. The present analysis is appropriate to large holes only, but the method of analysis given in MONZ can be adapted to consider these pressure-varying axisymmetric sausage modes for all hole sizes, when $\delta = 0$. An account of this has been given by Michael & O'Neill, and appears as an appendix to this paper.

## 5. Conclusion

The authors have been able to obtain numerically the loci of axisymmetric solutions at prescribed values of $\delta$. Typical results are shown in figures 3, 4 and 5 for the values $\delta = -0{\cdot}2$, 0 and $+0{\cdot}2$ respectively. In each case the point $A$ is the

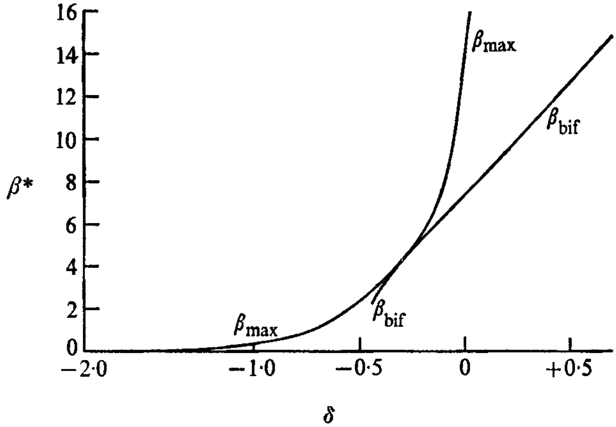


FIGURE 6. The value $\beta = \beta^*$ at the first instability, for varying $\delta$. $\beta_{max}$ denotes the value of $\beta$ at the first maximum of the symmetric loci in the $\alpha$, $\beta$ plane. $\beta_{bif}$ denotes the value of $\beta$ at the first asymmetric bifurcation. The critical value $\beta^* = \beta_{max}$ for $\delta < -0{\cdot}3$ approximately, and $\beta^* = \beta_{bif}$ for $\delta > -0{\cdot}3$.

equilibrium position before application of the electric field. For $\delta < 0$ the first branch, starting at $A$, is a centre-down branch which goes into the spiral point $C$ representing the centred cusp limit, as shown in figure 3. For $\delta > 0$ (figure 5), the branch starting from $A$ is a centre-up branch, and cannot connect with the spiral point $C$. In the marginal case $\delta = 0$, figure 4 shows the first symmetric bifurcation point $D$ on the straight-line locus $AE$. Below $D$ the bifurcated solution is a centre-down locus terminating at the cusp $C$. Above $D$ the bifurcation is a centre-up solution. This locus recrosses the line $AE$ but the solution is distinct from $y \equiv 1$, and the point is not a point of bifurcation. For the purpose of correlating figure 4 with figures 3 and 5 the branches $AD$ and $DE$ of figure 4 may be thought of as either centre-up or centre-down solutions. To correlate with figure 3, $AD$ is centre-down and $DE$ is centre-up, and vice versa for figure 5.

The most useful information to obtain from this analysis is the critical value $\beta = \beta^*$ at which the equilibrium will first become unstable, as a function of $\delta$. The calculation of this follows the pattern of the two-dimensional case in part 1. It normally occurs at the first asymmetric bifurcation point $B$. However as $\delta$ decreases we find, as in part 1, that $B$ reaches the maximum of $\beta$ on the first branch at $\delta = -0{\cdot}3$ approximately. For lower values of $\delta$ the maximum of $\beta$ is reached before the point $B$. Thus for $\delta > -0{\cdot}3$ the instability is an asymmetric one of the type observed in the experiments of Zuercher when $\delta = 0$. For $\delta < -0{\cdot}3$ the instability becomes an axisymmetric one at the point of maximum $\beta$. The values of $\beta^*$ have been calculated for a range of values of $\delta$, and are shown in figure 6.

The authors are grateful to Miss S. M. Burrough for her assistance with numerical calculations in parts 1 and 2 of this work. J. Norbury thanks the Science Research Council for a grant enabling him to visit New York, and the

United States Air Force Office of Scientific Research for computational facilities provided under grant AFOSR-71-2013. M. E. O'Neill wishes to acknowledge support from The National Research Council of Canada in the course of this work.

## Appendix. Axisymmetric sausage mode instability when $\delta = 0$

By D. H. MICHAEL and M. E. O'NEILL

The analysis given in MONZ proceeded on the assumption that small perturbations in the electric stress and surface-tension stress are exactly in balance at the point of instability, which leads to the conclusion that an axisymmetric sausage mode of instability cannot occur without violating the volume conservation requirement of incompressibility. It furthermore implies that it is not possible for the dielectric fluid to have an equilibrium profile shape which corresponds to an axisymmetric sausage mode of displacement. However, the foregoing discussion suggests that such modes are associated with changes in the internal static pressure, and this has prompted us to consider the problem again when a change in pressure is allowed to occur in the displacement of the system.

As in MONZ, we present two theoretical models for the perturbation of the system. The first is a simple approximate theory which ignores any coupling of the perturbation electric fields in the solid and liquid dielectrics. This, however, leads to discontinuities in both the perturbation potential and the normal component of the displacement vector across the wall $r = R$ although of small order of magnitude. The second theoretical model is exact and takes into account the coupling of the fields in the two dielectric phases.

### *Approximate and exact models for the perturbation*

When a change in the static pressure difference across the interfaces is allowed, an axisymmetric sausage mode displacement can be constructed in the following way. Using the configuration and notation given previously in MONZ, we consider a sausage mode of displacement in which the surface elevation $\zeta$ of the interface $z = h$ $(0 \leqslant r \leqslant R)$ is given by

$$\zeta = J_0(kr) - J_0(kR).$$

This form of displacement satisfies the condition that $\zeta = 0$ at $r = R$, and, in order to satisfy the volume conservation condition, it is necessary that

$$\int_0^R r\zeta\, dr = \int_0^R r[J_0(kr) - J_0(kR)]\, dr = 0.$$

This imposes a condition on the wavenumber $k$ such that

$$2J_1(kR) - kRJ_0(kR) = 0.$$

From Abramovitz & Stegun (1965, p. 414), the smallest value of $k$ satisfying this equation occurs when $kR \approx 5{\cdot}136$.

Corresponding to this form for $\zeta$ the perturbation electrostatic potential $\chi$ for a sausage mode has the form

$$\chi = -E_0\left\{\frac{\sinh kz}{\sinh kh} J_0(kr) - \frac{z}{h} J_0(kR)\right\}. \tag{A 1}$$

This satisfies Laplace's equation within the dielectric fluid and the surface condition that $\chi = \mp E_0 \zeta$ at $z = \pm h$ respectively. On the surface, which in the unperturbed state is $z = h$, the total stress is

$$(KE_0^2/4\pi h)\{kh \coth kh J_0(kr) - J_0(kR)\} \tag{A 2}$$

to first order. The constant term in (A 2) arises from the second term of (A 1).

In the marginal state the first term in (A 2) balances the surface-tension stress to give rise to the dispersion relation

$$KE_0^2 h/4\pi T = kh \tanh kh, \tag{A 3}$$

which is the same as that given previously for the sausage modes considered in MONZ. The second term of (A 2) shows that such a mode of disturbance must be accompanied by a small first-order increase $\delta p$ in the static pressure inside the dielectric fluid. This will be given by

$$\delta p = (-KE_0^2/4\pi h)\, J_0(kR).$$

Substitution of the value $kR = 5{\cdot}136$ into (3) gives a higher value of the applied field $E_0$ for instability of this mode than is necessary for the $S1$ mode given previously in MONZ, for which $kR \approx 3{\cdot}832$. Thus the instability of the axisymmetric sausage mode should not enter the correlation of theoretical and experimental results for the critical voltage.

However, in this simple model for the perturbation, we have ignored any change in the electric field inside the solid dielectric; we note that $\chi \neq 0$ and $\partial\chi/\partial r \neq 0$ for all $|z| < h$ along $r = R$. Thus there is a discontinuity at the wall $r = R$ in both the perturbation electrostatic potential and the displacement vector, the latter discontinuity implying that there is a layer of free charge between the solid and liquid dielectrics, which, as was pointed out in MONZ, did not occur in Zuercher's experiments.

It therefore remains for us to examine how far the conclusions which may be drawn using the simple model present an accurate description of the most unstable modes and, to do this, we present an exact theory which takes into account the coupling of the electric fields within the two dielectric phases. We shall assume that the dielectric constants $K$ for both the solid and liquid dielectric are equal as this case closely matches the situation in the experiments described in MONZ.

For an axisymmetric sausage mode, we write, following the notation of MONZ,

$$\zeta = \sum_{i=1}^{\infty} \zeta_{0i} J_0(\alpha_{0i} r) \quad (r \leqslant R),$$

where the $\alpha_{0i}$ denote the roots of $J_0(\alpha_{0i} R) = 0$. The condition of constancy of volume requires that

$$\int_0^R r\zeta\, dr = -\sum_{i=1}^{\infty} (\zeta_{0i}/\alpha_{0i})\, RJ_1(\alpha_{0i} R) = 0. \tag{A 4}$$

A suitable representation of $\chi$ within the strip $|z| < h$, $0 \leqslant r < \infty$ is given by

$$\chi = -E_0 \int_0^\infty F(k)\, k \frac{\sinh kz}{\sinh kh} J_0(kr)\, dk.$$

The boundary condition on $\chi$ requires that $\chi = \mp E_0\zeta$ for $0 \leqslant r \leqslant R$ and $\chi = 0$ for $r > R$ when $z = \pm h$.

Thus

$$F(k) = \int_0^R r\zeta J_0(kr)\,dr = \sum_{i=1}^{\infty} \zeta_{0i} F_{0i},$$

where

$$F_{0i} = -\frac{\alpha_{0i} R}{k^2-\alpha_{0i}^2} J_0(kR)\, J_1(\alpha_{0i} R).$$

Consequently,

$$\chi = -E_0 \int_0^\infty k \frac{\sinh kz}{\sinh kh} \sum_{i=1}^{\infty} \zeta_{0i} F_{0i}(k)\, J_0(kr)\,dk.$$

The surface stress condition, when allowance is made for a small increase $\delta p$ in the pressure within the dielectric fluid over that of the conducting fluids, now takes the form

$$T\left(\frac{\partial^2\zeta}{\partial r^2}+\frac{1}{r}\frac{\partial\zeta}{\partial r}\right)+\delta p = \frac{KE_0}{4\pi}\frac{\partial\chi}{\partial z}, \quad |z| = h, \tag{A 5}$$

when $r \leqslant R$. We can express each of the terms of (A 5) as a series involving the complete set of orthogonal functions $J_0(\alpha_{0i} r)$ $(i = 1, 2, \ldots)$.

Therefore we have

$$T\left(\frac{\partial^2\zeta}{\partial r^2}+\frac{1}{r}\frac{\partial\zeta}{\partial r}\right) = -T\sum_{i=1}^{\infty} \alpha_{0i}^2 \zeta_{0i} J_0(\alpha_{0i} r),$$

and noting that, for $0 \leqslant r < R$,

$$J_0(kr) = -\frac{2}{R}\sum_{j=1}^{\infty} \frac{\alpha_{0j} J_0(kR)\, J_0(\alpha_{0j} r)}{(k^2-\alpha_{0j}^2)\, J_1(\alpha_{0j} R)},$$

it follows that, for $|z| = h$,

$$\frac{KE_0}{4\pi}\frac{\partial\chi}{\partial z} = \frac{KE_0^2}{2\pi R}\sum_{i,j=1}^{\infty} \alpha_{0j}\zeta_{0i}\frac{J_0(\alpha_{0j} r)}{J_1(\alpha_{0j} R)}\int_0^\infty \frac{F_{0i}(k)\, J_0(kR)\, k^2 \coth kh}{(k^2-\alpha_{0j})^2}\,dk. \tag{A 6}$$

It is also easy to show that

$$\delta p = \frac{2\delta p}{R}\sum_{j=1}^{\infty} \frac{J_0(\alpha_{0j} R)}{\alpha_{0j} J_1(\alpha_{0j} R)} \quad (0 \leqslant r < R).$$

In order to satisfy (A 5) for all $r$ in the range $0 \leqslant r < R$ it is essential that the coefficients of $J_0(\alpha_{0j} r)$ on either side of the equation are the same. It therefore follows that

$$-T\alpha_{0j}^2\zeta_{0j} + \frac{2\delta p}{R\alpha_{0j} J_1(\alpha_{0j} R)} = \frac{KE_0^2}{2\pi R}\sum_{i=1}^{\infty}\frac{\alpha_{0j}\zeta_{0i}\mathscr{C}_{ij}}{J_1(\alpha_{0j} R)},$$

with $\mathscr{C}_{ij}$ denoting the integral occurring in (A 6). This determines the following set of linear equations for the coefficients $\zeta_{0j}$:

$$\sum_{i=1}^{\infty}\frac{\zeta_{0i}}{\alpha_{0i}} J_1(\alpha_{0i} R) = 0, \tag{A 7}$$

which follows immediately from (A 4), together with

$$\frac{KE_0^2}{2\pi R}\sum_{i=1}^{\infty}\frac{\alpha_{0j}\zeta_{0i}\mathscr{C}_{ij}}{J_1(\alpha_{0j} R)} + T\alpha_{0j}^2\zeta_{0j} = \frac{2\delta p}{R\alpha_{0j} J_1(\alpha_{0j} R)}, \tag{A 8}$$

with $j = 1, 2, \ldots$.

If we now write $\mu = 2\pi T/KE_0^2 h$, $\nu = 4\pi\delta p/KE_0^2$, $x = kh$, $a = R/h$ and $Y_i = \alpha_{0i} J_1(\alpha_{0i} R)\zeta_{0i}$ and let $\xi_i$ $(i = 1, 2, \ldots)$ denote the roots of $J_0(\xi) = 0$, equation (A 8) reduces to the dimensionless form

$$\sum_{j=1}^{\infty} C_{ij} Y_j - \mu Y_i = \nu a/\xi_i^2 \quad (i = 1, 2, 3, \ldots), \tag{A 9}$$

where

$$C_{ij} = \int_0^\infty \frac{x^2 \coth x [J_0(ax)]^2 \, dx}{(x^2 - \xi_i^2/a^2)(x^2 - \xi_j^2/a^2)}. \tag{A 10}$$

Equation (A 7) reduces to

$$\sum_{i=1}^{\infty} (\xi_i)^{-2} Y_i = 0. \tag{A 11}$$

Our problem is therefore to find the largest (positive) value $\mu_{\max}$ of $\mu$ which is such that the inhomogeneous system of linear equations

$$\{\mathbf{C} - \mu \mathbf{I}\}\mathbf{Y} = \nu a \mathbf{A} \tag{A 12}$$

has a solution subject to the constraint

$$\mathbf{A}.\mathbf{Y} = 0, \tag{A 13}$$

where $\mathbf{C} = \{C_{ij}\}$, $\mathbf{I} = \{\delta_{ij}\}$, $\mathbf{A} = (\xi_1^{-2}, \xi_2^{-2}, \ldots)^{\mathrm{T}}$

and $\mathbf{Y} = (Y_1, Y_2, \ldots)^{\mathrm{T}}$.

If we assume that the solution of (A 12) and (A 13) can be regarded as the limit of the solution of the corresponding finite $n \times n$ system of equations as $n \to \infty$, we can proceed to determine $\mu_{\max}$ in the following way. Because $\mathbf{C}$ is real and symmetric, it has, when truncated to an $n \times n$ matrix, $n$ real and distinct eigenvalues $\lambda_1, \lambda_2, \ldots, \lambda_n$, which we shall suppose are such that $\lambda_1 > \lambda_2 > \ldots > \lambda_n$. If the corresponding orthonormal eigenvectors are $\mathbf{u}_1, \mathbf{u}_2, \ldots, \mathbf{u}_n$, the solution $\mathbf{Y}$ may be written as

$$\mathbf{Y} = y_1 \mathbf{u}_1 + y_2 \mathbf{u}_2 + \ldots + y_n \mathbf{u}_n.$$

Thus (A 12) gives

$$\sum_{i=1}^{n} (\lambda_i - \mu) y_i \mathbf{u}_i = \nu a \mathbf{A},$$

which implies that

$$(\lambda_i - \mu) y_i = \nu a \mathbf{A}.\mathbf{u}_i,$$

and because of the constraint (A 13)

$$\sum_{i=1}^{n} \frac{(\mathbf{A}.\mathbf{u}_i)^2}{\lambda_i - \mu} = 0. \tag{A 14}$$

It is easy to show that (A 14) has $n-1$ roots which interlace the eigenvalues $\lambda_1, \lambda_2, \ldots, \lambda_n$. Thus the largest root of (A 14) will be less than the largest eigenvalue of $\mathbf{C}$ when truncated to order $n$.

The (approximate) value of $\mu_{\max}$ for a given value of $a$ was found by solving (A 14) for increasing values of $n$ until agreement to at least three significant figures was achieved with two successive values of $n$. In practice we found that over the range of values of $a$ considered, namely $0{\cdot}1 \leqslant a \leqslant 8{\cdot}0$, the value of $n$ did not need to exceed $n = 6$ in order to obtain the desired accuracy. In table 1 we list the values

| $a$ | $\mu_{max}$ | $\lambda_{max}$ | $\mu^*$ |
|---|---|---|---|
| 0·1 | 0·00925 | 0·0121 | 0·00974 |
| 0·2 | 0·0185 | 0·0242 | 0·0195 |
| 0·4 | 0·0370 | 0·0485 | 0·0389 |
| 0·6 | 0·0555 | 0·0728 | 0·0584 |
| 0·8 | 0·0741 | 0·0973 | 0·0779 |
| 1·0 | 0·0927 | 0·122 | 0·0974 |
| 2·0 | 0·190 | 0·262 | 0·197 |
| 4·0 | 0·447 | 0·694 | 0·454 |
| 6·0 | 0·836 | 1·382 | 0·842 |
| 8·0 | 1·371 | 2·339 | 1·376 |

TABLE 1

of $\mu_{max}$ over this range of values of $a$. The quantity with which $\mu_{max}$ must be compared is the value of $\lambda_{max}$ calculated in MONZ for the $S1$ sausage mode, and it will be seen from the table that $\lambda_{max}$ exceeds $\mu_{max}$ throughout the range of $a$, thus indicating that the $S1$ sausage mode considered in MONZ becomes unstable at a *lower* field strength than does the $S0$ sausage mode considered in this paper. For completeness we have also displayed in the table the value of $\mu^*$ which for a given value of $a$ represents the value of $\mu$ corresponding to $\mu_{max}$ derived from the simple model discussed earlier when the conditions of continuity of the potential and the normal component of the displacement vector at $r = R$ are not satisfied. From (A 3), the expression for $\mu^*$ is accordingly given by

$$\mu^* = (a/2\zeta_1)\coth(\zeta_1/a), \tag{A 15}$$

where $\zeta_1 \approx 5{\cdot}136$ is the smallest non-zero root of

$$2J_1(\zeta) - \zeta J_0(\zeta) = 0.$$

The method of determining the eigenvalues of $\mathbf{C}$ is described in MONZ and will not be repeated here except to say that the size of the truncated $n \times n$ matrix is now determined such that $\mu_{max}$ is evaluated correct to at least three significant figures.

The foregoing analysis has shown that the $S0$ axisymmetric sausage mode of disturbance, though physically possible when there is a change of $\delta p$ in the static pressure when the equilibrium of the system is perturbed, is not the most unstable mode. However it is of interest to consider also why it is that, when $\delta p$ is non-zero, such a variation in the stability analysis is appropriate *only* for the axisymmetric sausage mode. Asymmetric modes, both of the sausage and kink types, can be ruled out because $\delta p$ cannot take on a $\sin m\theta$ or $\cos m\theta$ variation, since it is at most a constant for a static disturbance. It therefore only remains for us to consider whether or not an axisymmetric kink mode has any significance in the stability analysis. In the simple model for the perturbation, the form of $\chi$ for an axisymmetric kink mode corresponding to (A 1) has a second term which is a constant, and this term therefore contributes nothing to the electrical surface stress. Consequently, since $\delta p$ can be at most a constant, it follows that $\delta p = 0$. Furthermore, in the exact model, we note that if we suppose that $\delta p \neq 0$ we are led to a system of linear equations analogous to (A 8) but without the constraint equivalent to (A 4), since in a kink mode disturbance the volume conservation condition is automatically satisfied. Thus no criterion for stability can be deduced when $\delta p \neq 0$. When $\delta p = 0$ the analysis of the axisymmetric kink mode given in MONZ is complete.

The work described in this appendix was completed while one of the authors (M. E. O'N.) was visiting the Department of Mathematics, University of Toronto, during which time he was supported by a grant from the National Research Council of Canada.

## REFERENCES

ABRAMOVITZ, M. & STEGUN, I. A. 1965 *Handbook of Mathematical Functions*. Dover.
ACKERBERG, R. C. 1969 *Proc. Roy. Soc.* A **312**, 129.
MICHAEL, D. H., NORBURY, J. & O'NEILL, M. E. 1974 *J. Fluid Mech.* **66**, 289.
MICHAEL, D. H., O'NEILL, M. E. & ZUERCHER, J. C. 1971 *J. Fluid Mech.* **47**, 609.
TAYLOR, G. I. 1968 *Proc. Roy. Soc.* A **306**, 423.